https://doi.org/10.5194/egusphere-2026-4526
Preprint. Discussion started: 20 August 2026

Influence of solar, solar wind, and geomagnetic activity on the ionospheric propagation factor M(3000)F2 over Ouagadougou in the African equatorial sector

Abdullahi Kikelomo Kazeem
Department of Physics, Edo State University, Iyamho, Edo State, Nigeria
Corresponding E-mail Address: k6abdul@yahoo.com
ORCID iD - 0000-0001-8531-8146

Abstract

This study examines how solar, solar wind, and geomagnetic activity influence the ionospheric propagation factor M(3000)F2 over Ouagadougou (12.4°N, 358.5°E; dip latitude +1.45°), an equatorial station in the African sector. Hourly ionosonde observations from 1976 to 1997, spanning Solar Cycles 21 and 22, were analysed to investigate diurnal, seasonal, solar cycle, and storm-time variability of M(3000)F2. Representative years of high (1991), moderate (1993), and low (1995) solar activity were selected for climatological analyses, while seven geomagnetic storm events were examined to assess storm-time responses. Relationships between annual mean M(3000)F2 and selected solar, solar wind, and geomagnetic parameters were evaluated using correlation and linear regression analyses. M(3000)F2 exhibits pronounced diurnal and seasonal variability, characterised by higher nighttime and early-morning values, lower daytime values, and distinct equinoctial and solstitial differences associated with equatorial electrodynamics and thermospheric dynamics. An inverse dependence on solar activity is observed, with the highest M(3000)F2 values occurring during solar minimum. The strongest correlation is with the solar radio flux F10.7 ($R = -0.810$, $R^2 = 0.657$, $p < 0.001$), followed by the interplanetary magnetic field magnitude (B) ($R = -0.689$, $R^2 = 0.475$, $p < 0.001$) and the disturbance storm time (Dst) index ($R = 0.527$, $R^2 = 0.277$, $p = 0.0117$). Relationships with the planetary (Ap) index, the southward component of the interplanetary magnetic field (Bz), solar wind dynamic pressure (Psw), and solar-wind speed (Vsw) are weak and not statistically significant. During geomagnetic storms, M(3000)F2 generally decreases during the daytime main phase and recovers within one to two days, depending on storm intensity and background ionospheric conditions. The results indicate that long-term variability of M(3000)F2 over the African equatorial sector is primarily controlled by solar activity, with geomagnetic disturbances providing secondary modulation during storm periods. These findings contribute to a better understanding of equatorial ionospheric variability and provide useful information for HF radio wave propagation, empirical ionospheric modelling, and space weather applications.

Keywords: M(3000)F2; Equatorial ionosphere; Solar activity; Geomagnetic activity.

1. Introduction

The ionosphere, extending through the Earth's upper atmosphere, is a dynamic plasma environment that strongly influences high-frequency (HF) radio wave propagation. Among its ionised layers, the F2 layer is the most important for long-distance radio communication because it usually possesses the highest electron density and persists throughout both daytime and nighttime. One of the principal parameters used to characterise HF propagation is the propagation factor M(3000)F2, defined as the ratio of the maximum usable frequency (MUF) over a 3000 km transmission path to the critical frequency of the F2 layer (foF2). Because M(3000)F2 is closely related to the peak height of the F2 layer (hmF2), it provides valuable information on the vertical structure of the ionosphere and remains an essential parameter for empirical ionospheric modelling, HF propagation prediction, and space weather applications (Dudeney, 1983; Bilitza, 2018; Bilitza et al., 2022).

Unlike electron density parameters such as foF2, M(3000)F2 primarily reflects variations in F-region height and propagation geometry rather than ionisation alone. Early investigations demonstrated that M(3000)F2 exhibits distinct solar cycle behaviour and is closely linked to changes in hmF2 (Bilitza et al., 1979). Kouris (1998) further showed that the solar cycle response of M(3000)F2 differs markedly from that of foF2 because the propagation factor is more sensitive to structural changes in the F2 layer than to electron-density variations. These studies

https://doi.org/10.5194/egusphere-2026-4526
Preprint. Discussion started: 20 August 2026

demonstrate that M(3000)F2 is an effective diagnostic parameter for investigating ionospheric dynamics and radio wave propagation.

Variability in the ionosphere is primarily controlled by solar radiative forcing. Extreme ultraviolet (EUV) radiation ionises the neutral atmosphere, while long-term solar activity is commonly represented by the F10.7 solar radio flux and sunspot number (SSN). Variations in solar activity modify electron production, thermospheric composition, plasma transport, and ionosphere-thermosphere coupling, producing significant changes in foF2, hmF2, and related ionospheric parameters (Rishbeth and Mendillo, 2001; Bilitza et al., 2022). Since M(3000)F2 depends strongly on hmF2, it is expected to exhibit pronounced solar cycle variability, albeit in the opposite direction to electron-density parameters such as foF2 (Kouris, 1998).

In addition to solar radiation, solar wind and geomagnetic activity influence the ionosphere through solar wind-magnetosphere-ionosphere coupling. Variations in the interplanetary magnetic field (IMF), particularly its southward component (Bz), together with changes in solar wind speed and dynamic pressure, regulate magnetospheric energy transfer and initiate geomagnetic storms. These disturbances generate prompt penetration electric fields (PPEFs), disturbance dynamo electric fields (DDEFs), and storm-induced thermospheric circulation that modify plasma transport, F-region height, and electron density (Fejer, 2002; Pedatella and Liu, 2020). At equatorial latitudes, these processes strongly influence the vertical E × B plasma drift, which governs the development of the F2 layer and the equatorial ionisation anomaly (Abdu et al., 1990). Consequently, geomagnetic storms can produce substantial perturbations in M(3000)F2 through changes in the vertical structure of the F region.

The African equatorial ionosphere exhibits distinctive features, including the equatorial electrojet, the equatorial ionisation anomaly, and strong ionosphere-thermosphere coupling. These processes produce pronounced diurnal, seasonal, and solar-cycle variability that differs from that in other longitudinal sectors. However, Africa remains one of the least instrumented regions for ionospheric observations, resulting in relatively few long-term climatological

https://doi.org/10.5194/egusphere-2026-4526
Preprint. Discussion started: 20 August 2026

studies. Ouagadougou (Burkina Faso), located near the magnetic equator, is one of the few African stations with a long, nearly continuous ionosonde record spanning more than three decades, making it particularly valuable for investigating long-term ionospheric variability and for validating empirical ionospheric models.

Previous investigations over Ouagadougou have primarily focused on the climatological characteristics of M(3000)F2 and its representation by empirical models (Oyekola and Fagundes, 2010, 2012), while other African studies have largely concentrated on parameters such as foF2, total electron content (TEC), or electron density. More recently, Kazeem et al. (2026a) demonstrated that the E-region peak electron density over Ouagadougou responds significantly to solar and geomagnetic forcing, highlighting the sensitivity of the African equatorial ionosphere to solar-terrestrial processes.

Despite these advances, several important gaps remain. Previous studies have rarely examined the combined influence of solar activity, solar wind parameters, and geomagnetic activity on M(3000)F2 using a long-term dataset spanning multiple solar cycles. Furthermore, few investigations have integrated climatological analyses with storm-time responses and with statistical relationships between M(3000)F2 and multiple geophysical drivers. Consequently, the relative contributions of solar irradiance, solar wind conditions, and geomagnetic activity to long-term M(3000)F2 variability over the African equatorial region remain poorly understood.

To the best of our knowledge, this study provides the first comprehensive investigation of the relationships between M(3000)F2 and solar activity, solar wind parameters, and geomagnetic forcing over Ouagadougou using a 22-year ionosonde dataset spanning Solar Cycles 21 and 22. Building on previous studies, it combines climatological, storm-time, correlation, and regression analyses within a unified framework to evaluate the relative contributions of solar activity (F10.7), solar wind parameters (B, Bz, Psw, and Vsw), and geomagnetic indices (Dst and Ap) to long-term variability in M(3000)F2. The analysis identifies the principal geophysical drivers governing M(3000)F2 over the African equatorial sector. It provides new observational evidence of how solar, solar wind, and geomagnetic

https://doi.org/10.5194/egusphere-2026-4526
Preprint. Discussion started: 20 August 2026

processes collectively influence ionospheric propagation. These findings contribute to a better understanding of equatorial ionospheric variability and provide a useful observational basis for HF radio wave propagation studies, empirical ionospheric modelling, and space weather applications in the data-sparse African sector.

2. Data and Method of Analysis

This study uses M(3000)F2 observations recorded by the IPS-42 ionosonde at Ouagadougou, Burkina Faso (12.4° N, 358.5° E; dip latitude +1.45°). The station is located close to the magnetic equator, within the trough region of the equatorial ionisation anomaly, and provides an important observational site for investigating equatorial ionospheric variability in the African sector. The ionosonde operated from June 1966 to February 1998. For the present analysis, data covering solar cycles 21 and 22 were considered. The scaled ionosonde parameters were obtained from the database of the École Nationale Supérieure de Télécommunications de Bretagne (ENST Bretagne), where the dataset is archived (Ouattara et al., 2009).

In addition to the ionosonde observations, several solar, solar wind, and geomagnetic indices were used to characterise external forcing conditions. These include the 10.7 cm solar radio flux (F10.7), the interplanetary magnetic field magnitude (B), the southward component of the interplanetary magnetic field (Bz), solar wind speed (Vsw), solar wind dynamic pressure (Psw), the disturbance storm time index (Dst), and the planetary geomagnetic index (Ap). These parameters were retrieved from the OMNI database maintained by NASA's Space Physics Data Facility (available at https://omniweb.gsfc.nasa.gov).

Daily M(3000)F2 values and the corresponding geophysical indices were first used to derive monthly and yearly mean values. The monthly mean, M, was calculated as

$$M = \frac{1}{n}\sum_{i=1}^{n} D_i \qquad (1)$$

https://doi.org/10.5194/egusphere-2026-4526
Preprint. Discussion started: 20 August 2026

where D_i represents the daily values (arithmetic mean over all hours), and n is the number of available observations within a given month. The yearly mean, A, was then obtained from the monthly averages as

$$A = \frac{1}{12}\sum_{i=1}^{12} M \qquad (2)$$

Seasonal variability was examined using a modified Lloyd seasonal classification (Eleman, 1973). The months were grouped into four categories: March equinox (March-April), June solstice (May-August), September equinox (September-October), and December solstice (November-February), following Rabiu et al. (2007) and Kazeem et al. (2020). This subdivision allows separate examination of the two equinoctial intervals, which may exhibit distinct electrodynamic and thermospheric characteristics at equatorial latitudes. Seasonal mean values of M(3000)F2 were computed from the corresponding monthly averages.

Years with less than 65% completeness were excluded from the statistical analysis to minimise bias from sparse sampling. The 65% threshold was considered sufficient to derive representative monthly and yearly mean values from the long-term dataset. To investigate solar cycle dependence, representative years spanning different levels of solar activity were selected based on the annual mean F10.7 solar radio flux and data availability (≥65%). The selected years were 1991 (high solar activity, HSA; F10.7 = 209 sfu), 1993 (moderate solar activity, MSA; F10.7 = 110 sfu), and 1995 (low solar activity, LSA; F10.7 = 77 sfu). These representative years were used to investigate the diurnal, monthly, seasonal, and geomagnetic storm-time variability of M(3000)F2.

The response of M(3000)F2 to geomagnetic disturbances was investigated through case studies of selected storm events. Geomagnetically quiet conditions were defined by Kp ≤ 3 and Ap ≤ 15, whereas disturbed conditions were identified by Kp ≥ 4 and Ap ≥ 16. Seven geomagnetic storm events occurring during the selected study period were analysed. For each event, the five International Quiet Days (IQDs) corresponding to the same month were identified,

https://doi.org/10.5194/egusphere-2026-4526
Preprint. Discussion started: 20 August 2026

and their hourly M(3000)F2 values were averaged to establish a quiet-day reference (QAVE). The storm-time response of M(3000)F2 during the initial, main, and recovery phases was then compared with this quiet-day baseline.

Storm phases were identified individually using the temporal evolution of the Dst index. The initial phase was defined as the interval from storm commencement to the onset of the rapid decrease in Dst; the main phase as the period of rapid Dst decline to the minimum Dst value; and the recovery phase as the interval during which Dst gradually returned towards quiet-time conditions. For storms with recovery periods extending beyond one day, each recovery day was analysed separately to examine the temporal evolution of M(3000)F2 towards its quiet-time state.

Because the Ouagadougou ionosonde data contain missing observations during the nighttime and early morning hours, the storm-time analysis was restricted to periods with sufficient daytime data coverage. Consequently, the investigation focuses on the daytime response of M(3000)F2 during each storm phase rather than the complete diurnal evolution. Storm events with substantial data gaps that prevented meaningful interpretation were excluded from the analysis, while minor gaps in otherwise reliable events were retained and are acknowledged in the discussion where appropriate. Also, the local-time range shown varies among storm events depending on the availability of ionosonde observations.

The percentage storm-time deviation of M(3000)F2 was quantified using the percentage difference;

$$\%\,\Delta M(3000)F2 = \frac{M(3000)F2_{storm} - M(3000)F2_{quiet,ave}}{M(3000)F2_{quiet,ave}} \times 100 \qquad (3)$$

where $M(3000)F2_{storm}$ denotes the M(3000)F2 during the storm day and represents the $M(3000)F2_{quiet,ave}$ average M(3000)F2 of the five selected quiet days.

The five most geomagnetically quiet and stormy days are shown in Table 1.

https://doi.org/10.5194/egusphere-2026-4526
Preprint. Discussion started: 20 August 2026

Table 1: Geomagnetic Quiet and Storm days.

Year	Quiet Day	Storm Day
1991	May 11, 18, 20, 12, 19	May 16-18
1991	November 27, 26, 28, 25, 12	November 8-11
1993	March 5, 26, 6, 31, 19	March 8-10
1993	April 27, 3, 2, 28, 26	April 4-7
1993	May 25, 23, 21, 24, 22	May 9-11
1995	March 21, 22, 7, 8, 19	March 11-13
1995	September 29, 18, 22, 1, 2	September 26-29

To quantify the dependence of M(3000)F2 on solar, solar wind, and geomagnetic forcing, correlation and regression analyses were performed. M(3000)F2 was treated as the dependent variable, while F10.7, Dst, Ap, B, Bz, Vsw, and Psw were considered as independent variables. The statistical relationship between M(3000)F2 and each geophysical parameter was evaluated using the linear regression model:

$$y = a + bx + e \tag{4}$$

was applied, where y represents the dependent variable (M(3000)F2, x denotes each geophysical parameter, a is the intercept, b is the regression coefficient (slope), and e is the residual error term.

Yearly mean values were adopted for the correlation and regression analyses because relationships based on daily or monthly averages are often weakened by short-term variability, day-to-day ionospheric fluctuations, and data gaps. The use of yearly means reduces transient variability and provides more robust estimates of long-term solar

https://doi.org/10.5194/egusphere-2026-4526
Preprint. Discussion started: 20 August 2026

and geomagnetic control of ionospheric parameters, as demonstrated in earlier studies (Klobuchar and Doherty, 1992; Bilitza, 2001; Kazeem et al., 2014, 2026a, 2026b).

3. Result

3.1 Diurnal variation of M(3000)F2.

Figure 1 illustrates contour distributions of M(3000)F2 as a function of local time and day of year for representative years of high solar activity (HSA, 1991), moderate solar activity (MSA, 1993), and low solar activity (LSA, 1995). Across all three years, M(3000)F2 shows pronounced diurnal and day-to-day variability throughout the year.

During the HSA year (Figure 1, left panel), M(3000)F2 generally attains its highest values between approximately 0000 and 0800 LT. Thereafter, the parameter decreases gradually, reaching relatively low values around local noon (1200 LT). Following midday, M(3000)F2 remains low until approximately 2000 LT for most days of the year. However, between day numbers 75 and 180, the low-value region extends into the nighttime hours, indicating enhanced seasonal variability during this period.

The MSA year (Figure 1, middle panel) exhibits a similar diurnal structure, with elevated values at night and in the early morning and reduced values during the daytime. However, the overall M(3000)F2 values are generally higher than those observed during the HSA year.

For the LSA year (Figure 1, right panel), the diurnal pattern remains similar to that of the HSA and MSA years. The lowest values occur mainly between 1200 and 1600 LT. After this period, M(3000)F2 gradually increases through the evening and into the night, reaching a maximum in the early morning hours before decreasing again after approximately 0800 LT.

Overall, the contour plots indicate that M(3000)F2 is consistently highest during the LSA year, intermediate during the MSA year, and lowest during the HSA year, suggesting an inverse dependence of M(3000)F2 on solar activity.

https://doi.org/10.5194/egusphere-2026-4526
Preprint. Discussion started: 20 August 2026

Figure 2 shows the monthly mean diurnal variations of M(3000)F2 for the HSA (Figure 2a, top panel), MSA (Figure 2a, bottom panel), and LSA (Figure 2b) years. A common diurnal pattern is evident under all solar activity conditions, characterised by high values during the nighttime and early morning hours and lower values during the daytime.

During the HSA year, M(3000)F2 reaches maximum values between approximately 0400 and 0700 LT and decreases steadily after sunrise to attain minimum values between about 1100 and 2100 LT. Thereafter, the parameter gradually increases throughout the evening and nighttime until the early morning maximum is reached.

The MSA and LSA years exhibit similar diurnal behaviour, although the magnitude of M(3000)F2 progressively increases from HSA through MSA to LSA. Consequently, the monthly mean values are highest during the LSA year, followed by the MSA year, and lowest during the HSA year.

Overall, the monthly mean diurnal variations confirm the persistence of a well-defined diurnal cycle in M(3000)F2, characterised by daytime minima and nighttime-to-early-morning maxima under all solar activity conditions.

https://doi.org/10.5194/egusphere-2026-4526
Preprint. Discussion started: 20 August 2026

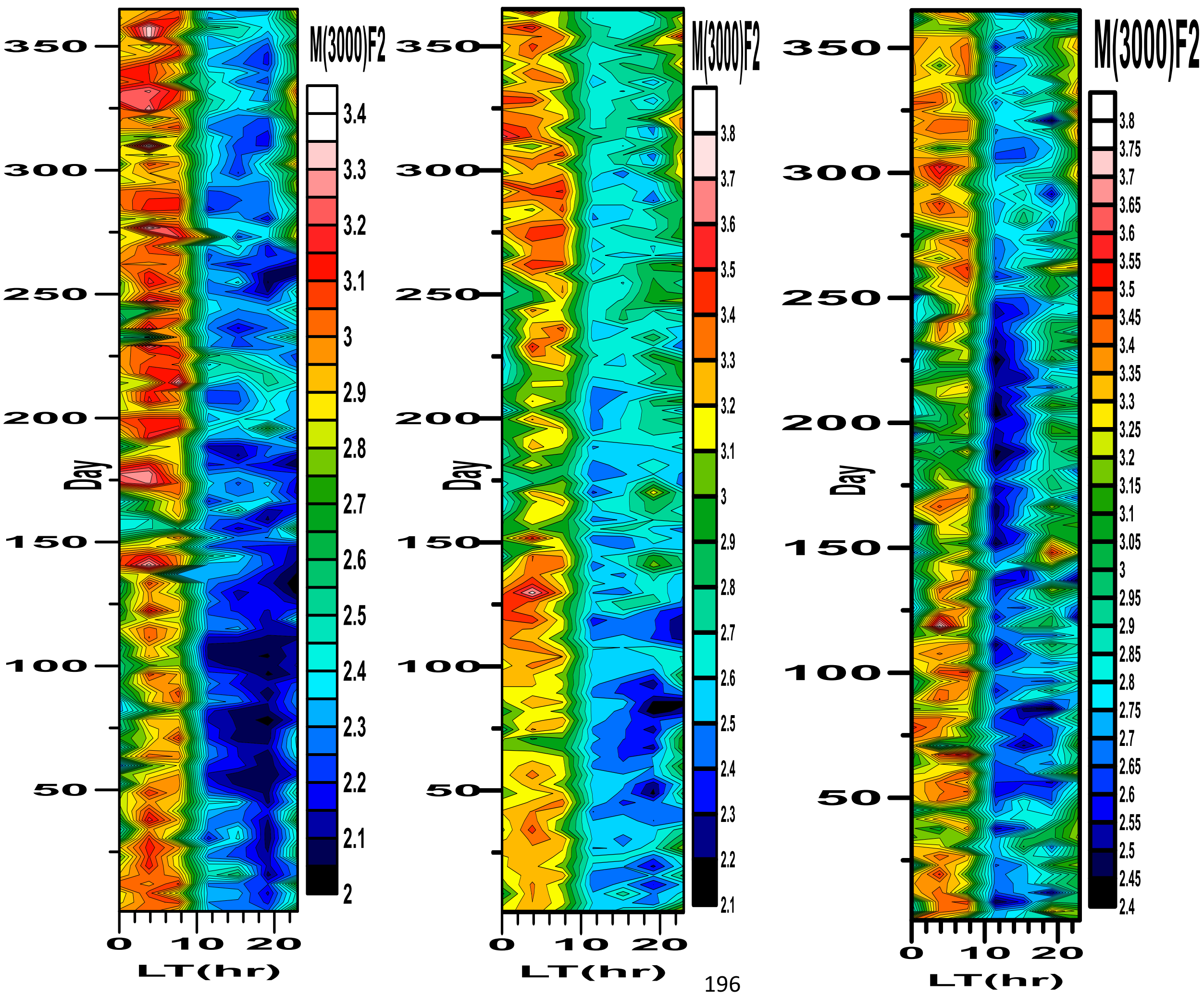

Figure 1 - Contour plot of M(3000)F2 versus day of the year and local time: left panel, 1991 (year of high solar activity); middle panel, 1993 (year of moderate solar activity); and right panel, 1995 (year of low solar activity).

https://doi.org/10.5194/egusphere-2026-4526
Preprint. Discussion started: 20 August 2026

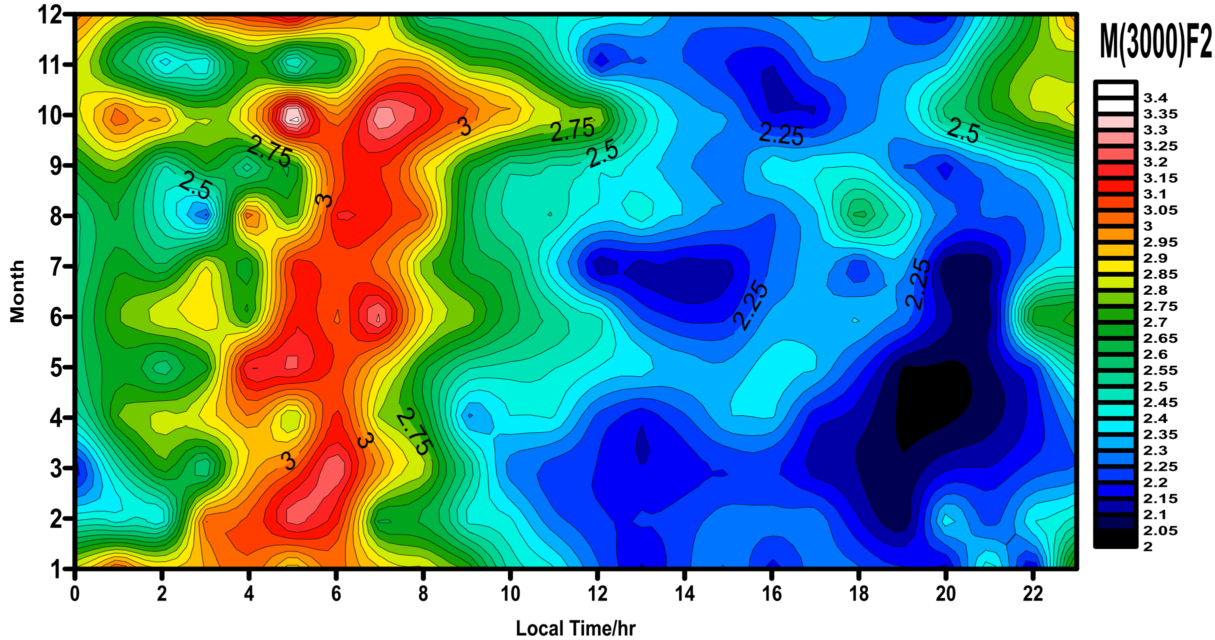

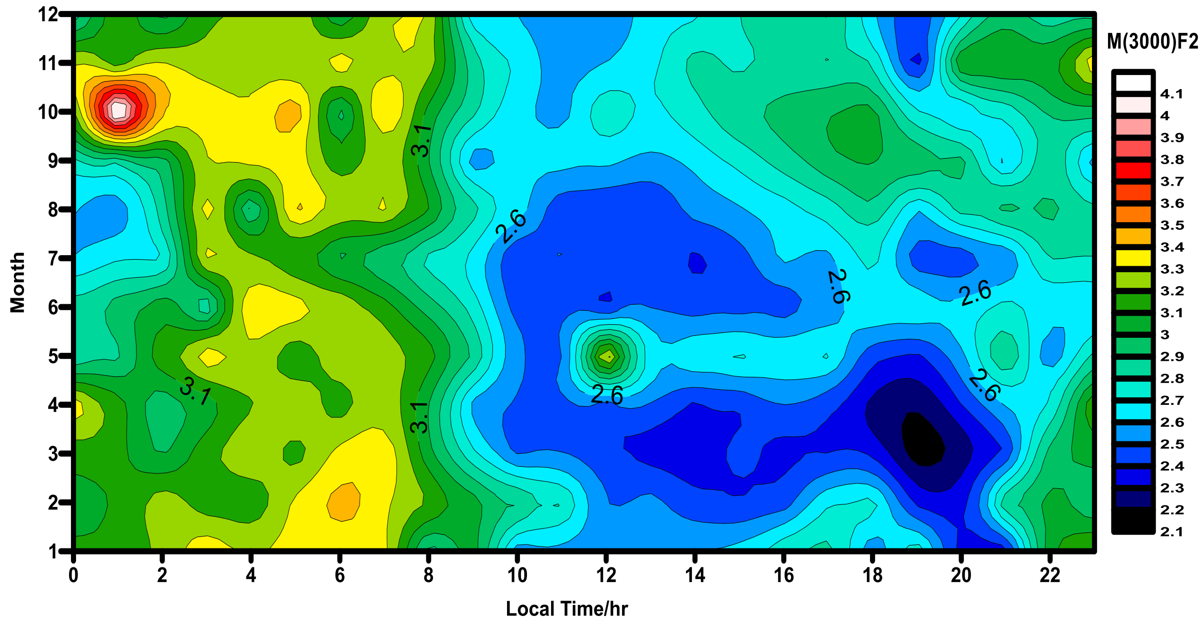

Figure 2a - Contour plot of M(3000)F2 showing month of the year versus local time: Top panel, 1991 (year of high solar activity). Bottom panel, 1993 (year of moderate solar activity).

https://doi.org/10.5194/egusphere-2026-4526
Preprint. Discussion started: 20 August 2026

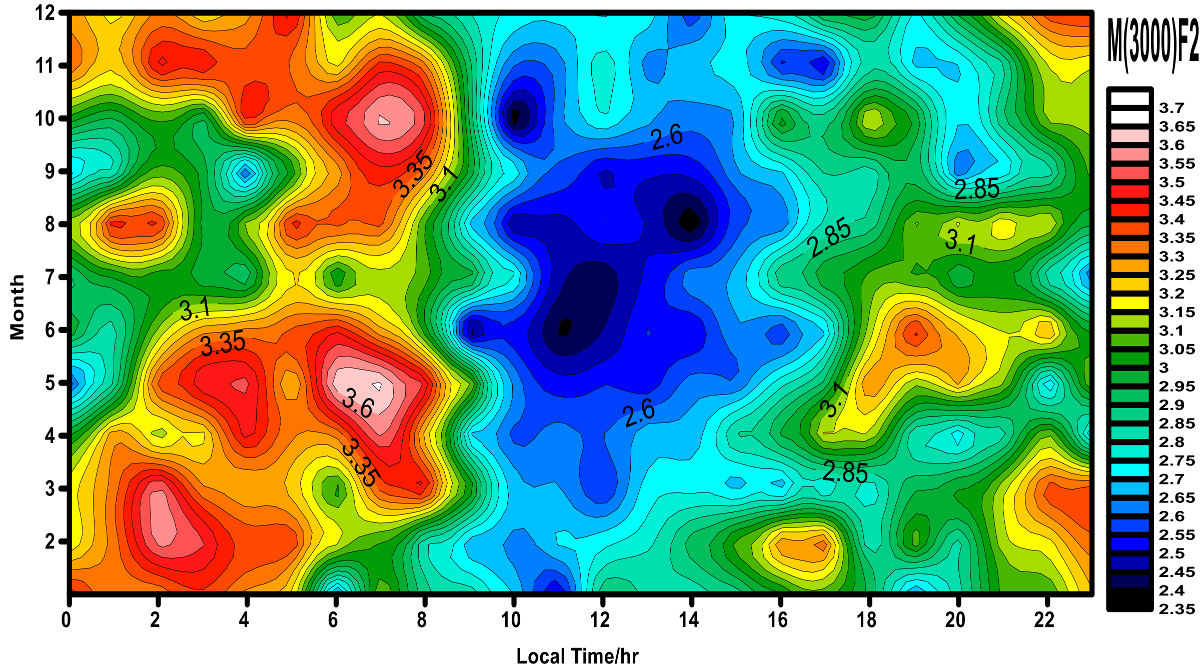

206

207 Figure 2b - Contour plot of M(3000)F2 showing the month of the year versus local time in 1995 (a year of low solar
208 activity).

209

210

211

212

213

214

215

https://doi.org/10.5194/egusphere-2026-4526
Preprint. Discussion started: 20 August 2026

3.2 Seasonal variation of M(3000)F2

Figure 3 and Table 2 present the seasonal mean values of M(3000)F2 over Ouagadougou for representative years of high (1991), moderate (1993), and low (1995) solar activity. The results indicate marked seasonal and interannual variability.

Across the three representative years, the highest seasonal mean M(3000)F2 values occur in the low solar activity year, followed by the moderate solar activity year, with the lowest values in the high solar activity year. This pattern indicates an inverse dependence of M(3000)F2 on solar activity.

During the high solar activity year (1991), M(3000)F2 reached its highest seasonal mean (1.7646) at the December solstice and its lowest (1.4404) at the June solstice. During the moderate solar activity year (1993), the seasonal mean increased from 1.4824 at the March equinox to 2.0356 at the September equinox, before decreasing slightly to 1.9764 at the December solstice. In the low solar activity year (1995), M(3000)F2 increased progressively from 1.9011 at the March equinox to a maximum of 2.1514 at the December solstice.

The seasonal distribution shows that the December solstice generally records the highest M(3000)F2 values, whereas the relative magnitudes of the March equinox, June solstice, and September equinox vary with the level of solar activity. These variations indicate that the seasonal behaviour of M(3000)F2 is influenced by both seasonal changes in equatorial ionospheric dynamics and the prevailing phase of the solar cycle.

https://doi.org/10.5194/egusphere-2026-4526
Preprint. Discussion started: 20 August 2026

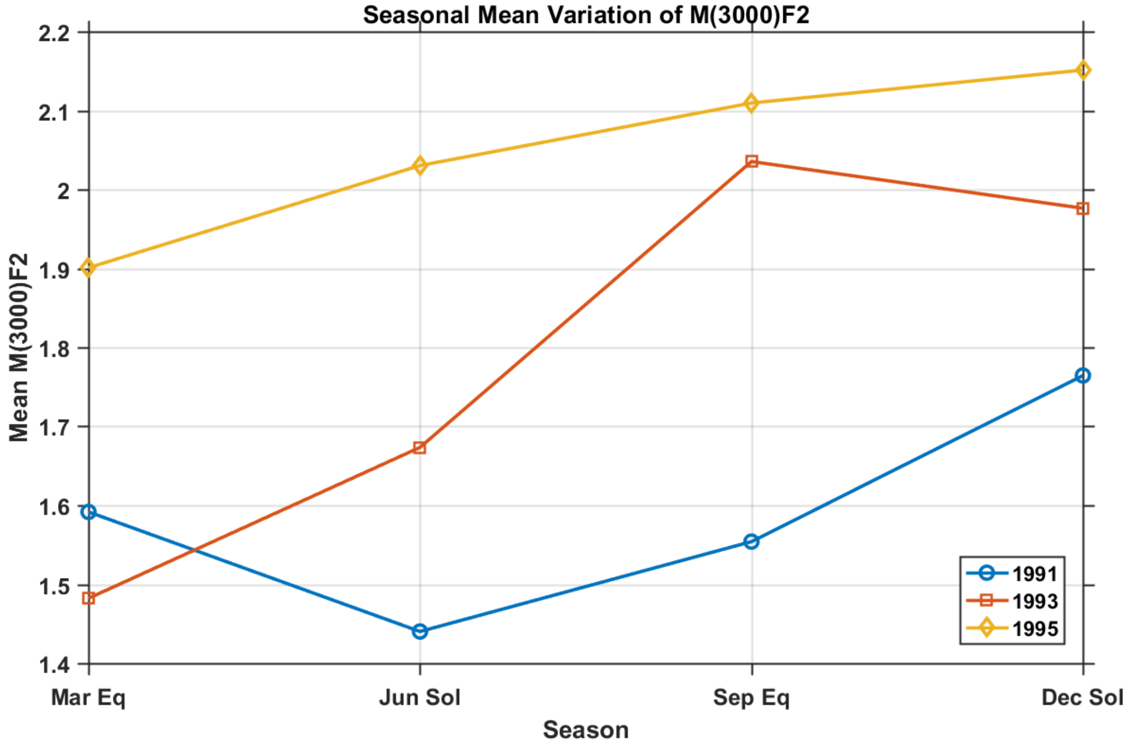

Figure 3- Seasonal variation of M(3000)F2 over Ouagadougou during the year of high solar activity (1991), the year of moderate solar activity (1993), and the year of low solar activity (1995)

https://doi.org/10.5194/egusphere-2026-4526
Preprint. Discussion started: 20 August 2026

Table 2: Summarises the seasonal mean values of M(3000)F2 for the representative years.

Season	HSA (1991)	MSA (1993)	LSA (1995)
March Equinox	1.5918	1.4824	1.9011
June Solstice	1.4404	1.6736	2.0305
September Equinox	1.5542	2.0356	2.1097
December Solstice	1.7646	1.9764	2.1514

https://doi.org/10.5194/egusphere-2026-4526
Preprint. Discussion started: 20 August 2026

3.3 Variation of M(3000)F2 and F10.7

Figure 4 compares the monthly variations of the ionospheric propagation factor M(3000)F2 and the solar radio flux (F10.7) over the period 1976-1997, encompassing Solar Cycles 21 (SC21) and 22 (SC22). Both parameters exhibit pronounced long-term variability associated with the solar cycle, although their temporal variations occur in opposite directions.

During SC21, M(3000)F2 increased from 1976 to a maximum monthly value of 3.11 in January 1977, after which it gradually decreased to a minimum value of 2.50 in March 1979. During SC22, M(3000)F2 reached its minimum monthly value of 2.40 in March 1991, then increased steadily to a maximum of 2.99 in December 1996.

The F10.7 solar radio flux exhibited the expected solar cycle variation. During SC21, F10.7 increased from a minimum value of 69 sfu in February 1976 to a maximum value of 229 sfu in May 1980. Similarly, during SC22, F10.7 reached its highest value of 247 sfu in June 1989, then declined progressively to a minimum of 70 sfu in February 1996.

Overall, the temporal variations indicate that periods of high F10.7 generally correspond to relatively low values of M(3000)F2, whereas periods of low F10.7 coincide with relatively high M(3000)F2 values, suggesting an inverse relationship between the two parameters over the study period.

https://doi.org/10.5194/egusphere-2026-4526
Preprint. Discussion started: 20 August 2026

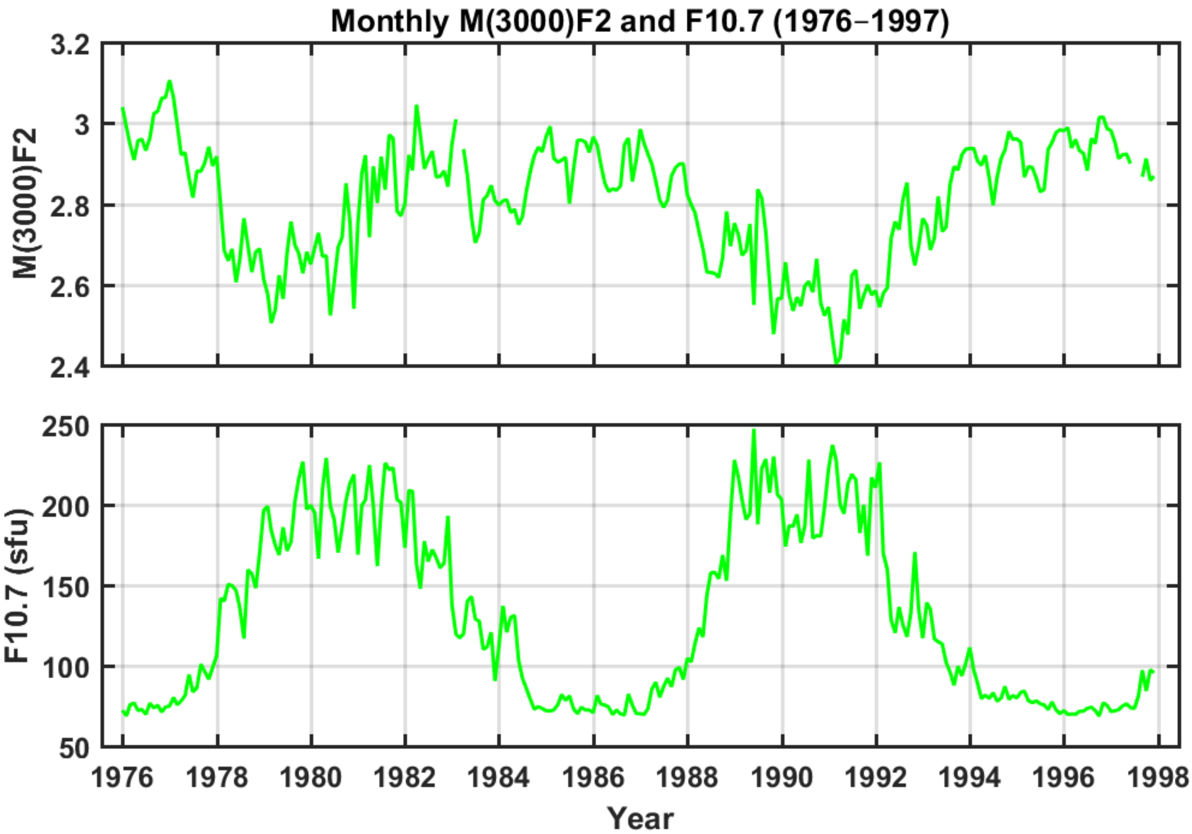

Figure 4- Variation of monthly average of M(3000)F2 (top panel) and F10.7 (bottom panel) in the period of 1976-1997.

https://doi.org/10.5194/egusphere-2026-4526
Preprint. Discussion started: 20 August 2026

3.4 Storm-time variation of M(3000)F2

The response of the equatorial ionospheric propagation factor, M(3000)F2, to geomagnetic storms is presented in this section. Seven geomagnetic storm events that occurred during the representative years 1991, 1993, and 1995 were analysed (Table 3). Based on the minimum Dst index following the classification of Gonzalez et al. (1994), the selected events comprised two moderate storms, four intense storms, and one super storm. Figures 5.1-5.7 illustrate the storm-time behaviour of M(3000)F2. In each figure, panel (a) presents the temporal evolution of the Dst index, while panel (b) compares the storm-time M(3000)F2 with the corresponding quiet-day average.

During the 16-18 May 1991 storm (Figure 5.1b), M(3000)F2 exhibited a pronounced depletion during the main phase, particularly between 0600 and 0900 LT, followed by a gradual recovery on the following day. The initial phase was characterised by modest afternoon enhancement, whereas the largest storm-time depletion (-26.4%) occurred at 0800 LT during the main phase. Recovery phase deviations were comparatively small, indicating that the ionosphere had begun returning toward quiet-time conditions.

For the 8-11 November 1991 super storm (Figure 5.2b), M(3000)F2 remained below the quiet-day average throughout most of the daytime during the main phase. Recovery extended over two days, with the first recovery day showing noticeable morning and afternoon enhancements before the parameter gradually approached the quiet-day profile during the second recovery day. The largest depletion (-21.5%) occurred during the main phase, while the strongest enhancement (15.5%) was recorded during the first recovery day.

The 8-10 March 1993 storm (Figure 5.3b) produced relatively small departures from quiet-time conditions during the initial phase. More pronounced variations occurred during the main phase, particularly during the late morning, with enhanced M(3000)F2 around 0800-0900 LT, followed by midday depletion. During the recovery phase, M(3000)F2 remained generally above the quiet-day average from 1000 to 1500 LT, indicating a relatively rapid recovery of the ionosphere.

For the 4-7 April 1993 storm (Figure 5.4b), the available observations indicate persistent depletion during the initial phase. Owing to data gaps, the main phase could not be evaluated. However, both recovery days showed gradual enhancement toward the quiet-day profile, with the second recovery day exhibiting the largest positive departures.

During the 9-11 May 1993 storm (Figure 5.5b), only modest variations were observed during the initial phase. In contrast, the main phase was characterised by a distinct reduction in M(3000)F2 between approximately 1100 and 1500 LT, with the maximum depletion reaching -8.1% at 1200 LT.

The 11-13 March 1995 storm (Figure 5.6b) produced relatively weak disturbances during the initial phase. The most significant response occurred during the main phase, when M(3000)F2 decreased during the afternoon hours, reaching a maximum depletion of -10.2% at 1600 LT. During the recovery phase, the parameter gradually approached the quiet-day values, although minor departures remained.

Similarly, the 26-29 September 1995 storm (Figure 5.7b) showed distinct storm-time variability throughout its evolution. Following modest morning enhancement during the initial phase, M(3000)F2 decreased markedly between approximately 1000 and 1600 LT during the main phase. Recovery extended over two days, with the first recovery day exhibiting stronger positive departures than the second, although complete recovery to quiet-time conditions was not achieved until the end of the event.

Overall, the analysed storm events consistently demonstrate that geomagnetic disturbances modify the diurnal behaviour of M(3000)F2, with the most pronounced perturbations generally occurring during the main phase of the storms. The response is characterised predominantly by daytime depletion, while recovery typically occurs gradually over one or two days, depending on storm intensity and duration.

https://doi.org/10.5194/egusphere-2026-4526
Preprint. Discussion started: 20 August 2026

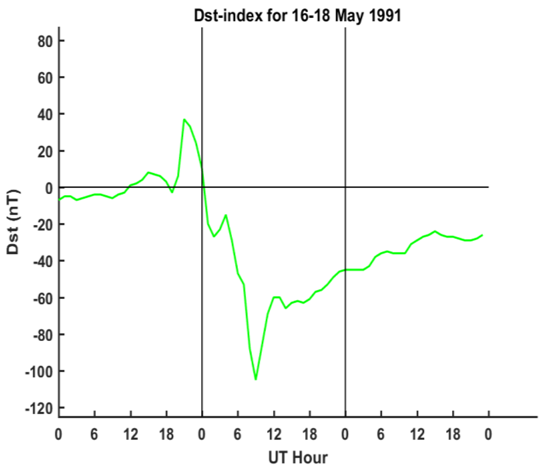

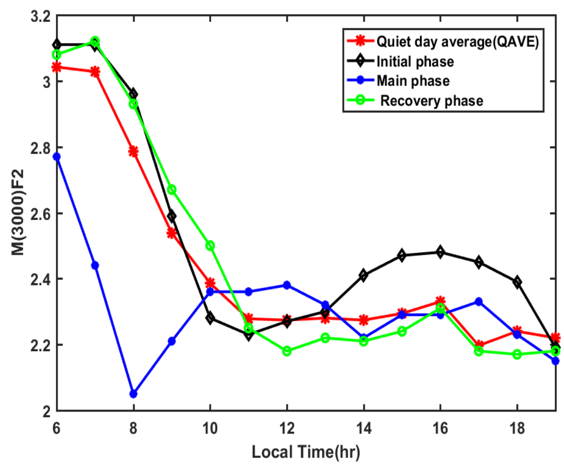

Figure 5.1a- Dst-Index plot for May 16-18, 1991. Figure 5.1b- Comparison of M(3000)F2 quiet-time average (May 1991) with the initial (16 May), main (17 May), and recovery (18 May) phases of the storm.

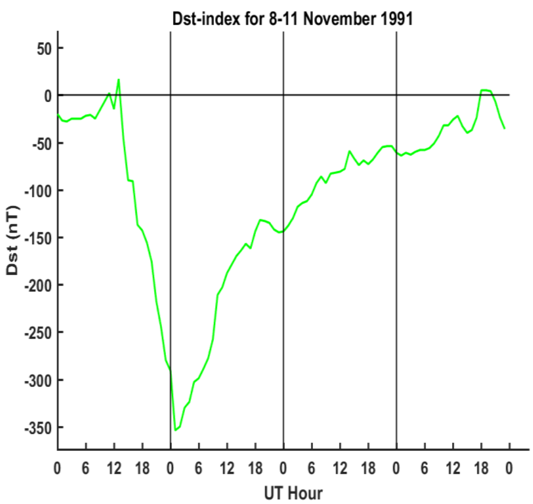

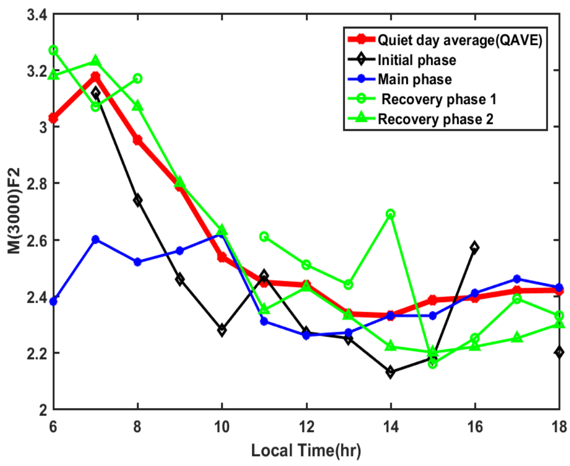

Figure 5.2a- Dst-Index plot for Nov. 8-11, 1991. Figure 5.2b- Comparison of M(3000)F2 quiet-time average (Nov. 1991) with the initial (8 Nov.), main (9 Nov.), recovery 1 (10 Nov.), and recovery 2 (11 Nov.) phases of the storm.

https://doi.org/10.5194/egusphere-2026-4526
Preprint. Discussion started: 20 August 2026

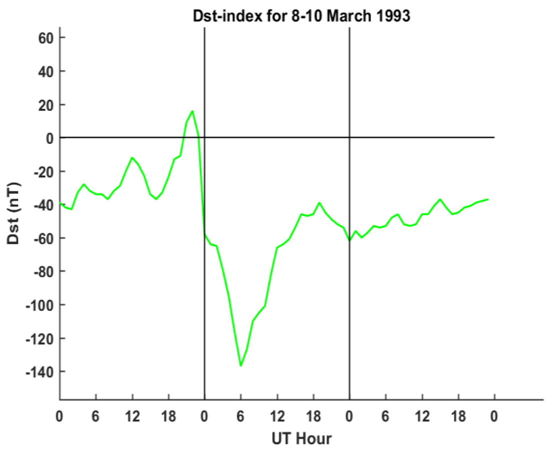

Figure 5.3a- Dst-Index plot for March 8-10, 1993.

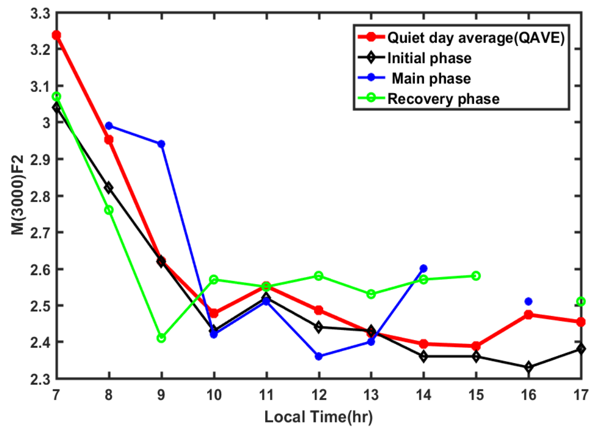

Figure 5.3b- Comparison of M(3000)F2 quiet-time average (Mar. 1993) with the initial (8 Mar.), main (9 Mar.), and recovery (10 Mar.) phases of the storm.

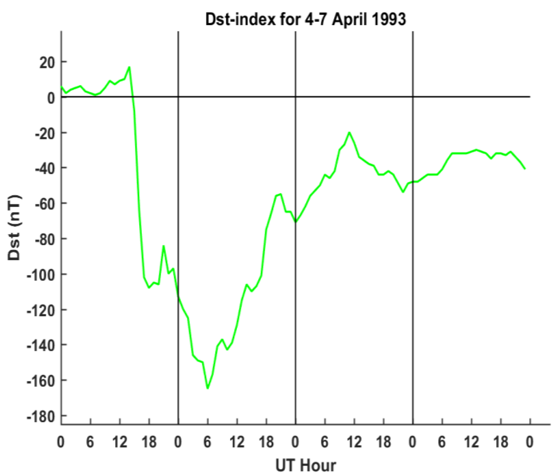

Figure 5.4a- Dst-Index plot for April 4-7, 1993.

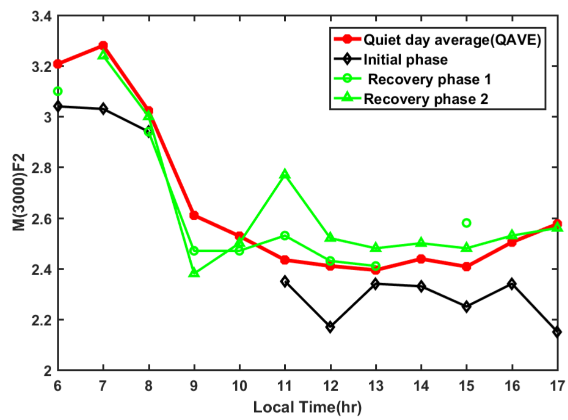

Figure 5.4b- Comparison of M(3000)F2 quiet-time average (April 1993) with the initial (4 April), recovery 1 (6 April), and recovery 2 (7 April) phases of the storm. The main phase is not shown because of missing ionosonde observations.

https://doi.org/10.5194/egusphere-2026-4526
Preprint. Discussion started: 20 August 2026

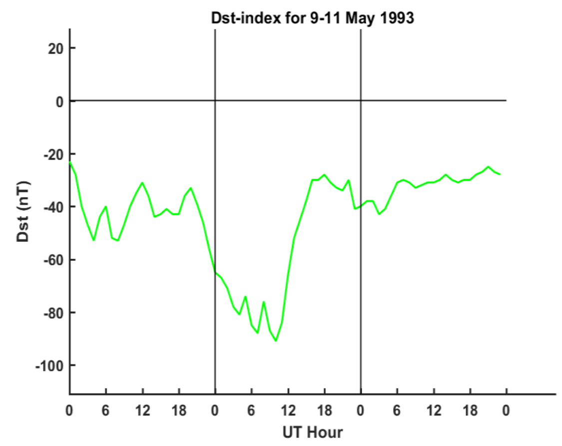

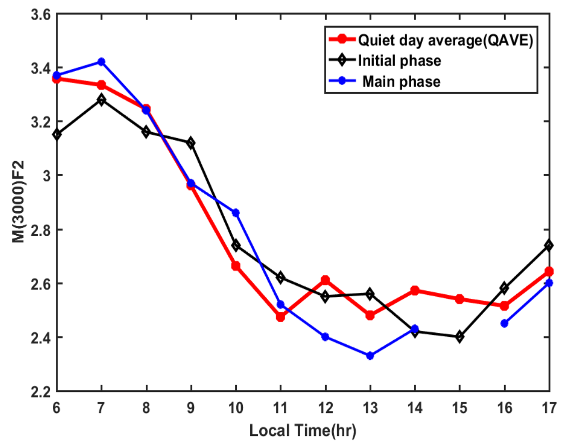

Figure 5.5a- Dst-Index plot for May 9-11, 1993.

Figure 5.5b- Comparison of M(3000)F2 quiet-time average (May 1993) with the initial (9 May) and main (10 May) phases of the storm. The recovery phase is not shown because of missing ionosonde observations.

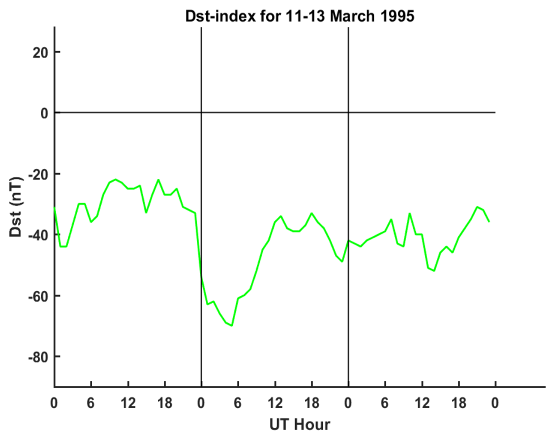

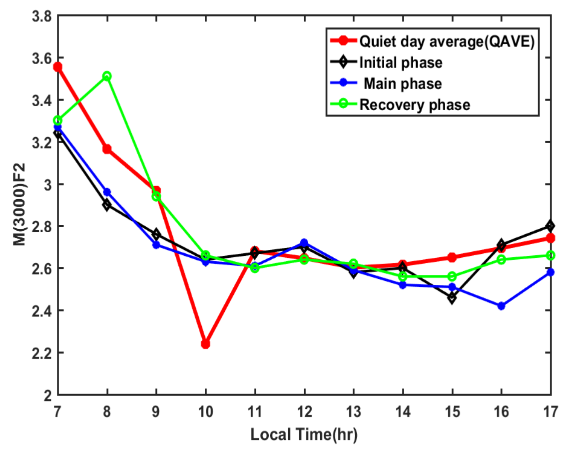

Figure 5.6a- Dst-Index plot for March 11-13, 1995

Figure 5.6- Comparison of M(3000)F2 quiet-time average (Mar. 1995) with the initial (11 Mar.), main (12 Mar.), and recovery (13 Mar.) phases of the storm.

https://doi.org/10.5194/egusphere-2026-4526
Preprint. Discussion started: 20 August 2026

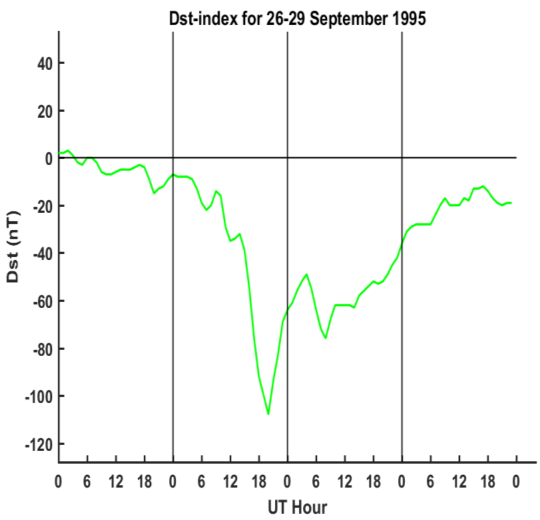

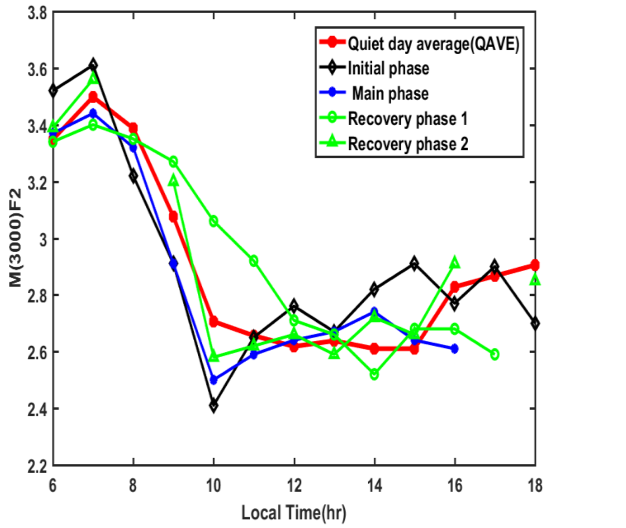

Figure 5.7a- Dst-Index plot for Sep.. 26-29, 1995. Figure 5.7b- Comparison of M(3000)F2 quiet-time average (Sep. 1991) with the initial (26 Sep.), main (27 Sep.), recovery (28 Sep.), and recovery 2 (29 Sep.) phases of the storm.

1

https://doi.org/10.5194/egusphere-2026-4526
Preprint. Discussion started: 20 August 2026

Table 3: Summary of the geomagnetic storm events and the observed M(3000)F2 response over Ouagadougou.

Storm event	Minimum Dst (nT)	Storm intensity	Storm phases analysed	Recovery duration	Dominant M(3000)F2 response
16-18 May 1991	-105	Intense	Initial, Main, Recovery	1 day	Morning depletion during the main phase
8-11 Nov 1991	-354	Super	Initial, Main, Recovery 1, Recovery 2	2 days	Daytime depletion and gradual recovery
8-10 Mar 1993	-137	Intense	Initial, Main, Recovery	1 day	Moderate daytime disturbance
4-7 Apr 1993	-165	Intense	Initial, Recovery 1, Recovery 2	2 days	Main phase unavailable due to data gaps
9-11 May 1993	-91	Moderate	Initial, Main	Recovery unavailable	Strong midday depletion
11-13 Mar 1995	-70	Moderate	Initial, Main, Recovery	1 day	Afternoon depletion and recovery
26-29 Sep 1995	-108	Intense	Initial, Main, Recovery 1, Recovery 2	2 days	Pronounced daytime depletion with gradual recovery

https://doi.org/10.5194/egusphere-2026-4526
Preprint. Discussion started: 20 August 2026

3.5 Relationship between M(3000)F2 and solar, solar wind, and geomagnetic activity

Relationships between yearly mean M(3000)F2 and the selected geophysical parameters were evaluated using correlation and linear regression analyses over the period 1976-1997, encompassing Solar Cycles 21 and 22. The relationships between M(3000)F2 and Dst, F10.7, Ap, B, Bz, Psw, and Vsw are presented in Figure 6, while the corresponding correlation coefficients (R), coefficients of determination (R^2), and *p*-values are summarised in Table 4.

The results indicate that M(3000)F2 exhibits varying degrees of correlation with the selected geophysical parameters. A moderate positive correlation was obtained between M(3000)F2 and Dst (R = 0.527, R^2 = 0.277), indicating that approximately 27.7% of the variability in M(3000)F2 is associated with variations in Dst. In contrast, M(3000)F2 shows a strong negative correlation with the solar radio flux F10.7 (R = -0.810, R^2 = 0.657), representing the strongest relationship among all the parameters considered. A moderate negative correlation was also observed between M(3000)F2 and the interplanetary magnetic field magnitude, B (R = -0.689, R^2 = 0.475), whereas the relationship with the planetary geomagnetic index, Ap, was weaker (R = -0.421, R^2 = 0.177). Comparatively weak relationships were obtained with the southward interplanetary magnetic field component, Bz (R = -0.270, R^2 = 0.073), the solar wind dynamic pressure, Psw (R = 0.141, R^2 = 0.020), and the solar wind speed, Vsw (R = 0.101, R^2 = 0.011).

The statistical significance of these relationships was evaluated using the corresponding *p*-values. At the 95% confidence level ($p < 0.05$), the *p*-values obtained were 4.9203×10^{-6} for F10.7, 3.9076×10^{-4} for B, 0.0117 for Dst, 0.0510 for Ap, 0.2243 for Bz, 0.5314 for Psw, and 0.6355 for Vsw. Accordingly, the relationships between M(3000)F2 and F10.7, B, and Dst are statistically significant, whereas those involving Ap, Bz, Psw, and Vsw are not statistically significant at the 95% confidence level.

https://doi.org/10.5194/egusphere-2026-4526
Preprint. Discussion started: 20 August 2026

Overall, the correlation coefficients range from -0.810 to 0.527, while the corresponding coefficients of determination range from 0.011 to 0.657. Among the investigated parameters, F10.7 exhibits the largest coefficient of determination (65.7%), followed by B (47.5%), Dst (27.7%), Ap (17.7%), Bz (7.3%), Psw (2.0%), and Vsw (1.1%). These results demonstrate that F10.7 has the strongest statistical relationship with M(3000)F2 over the study period, followed by B and Dst, while the remaining solar wind and geomagnetic parameters show comparatively weaker associations.

https://doi.org/10.5194/egusphere-2026-4526
Preprint. Discussion started: 20 August 2026

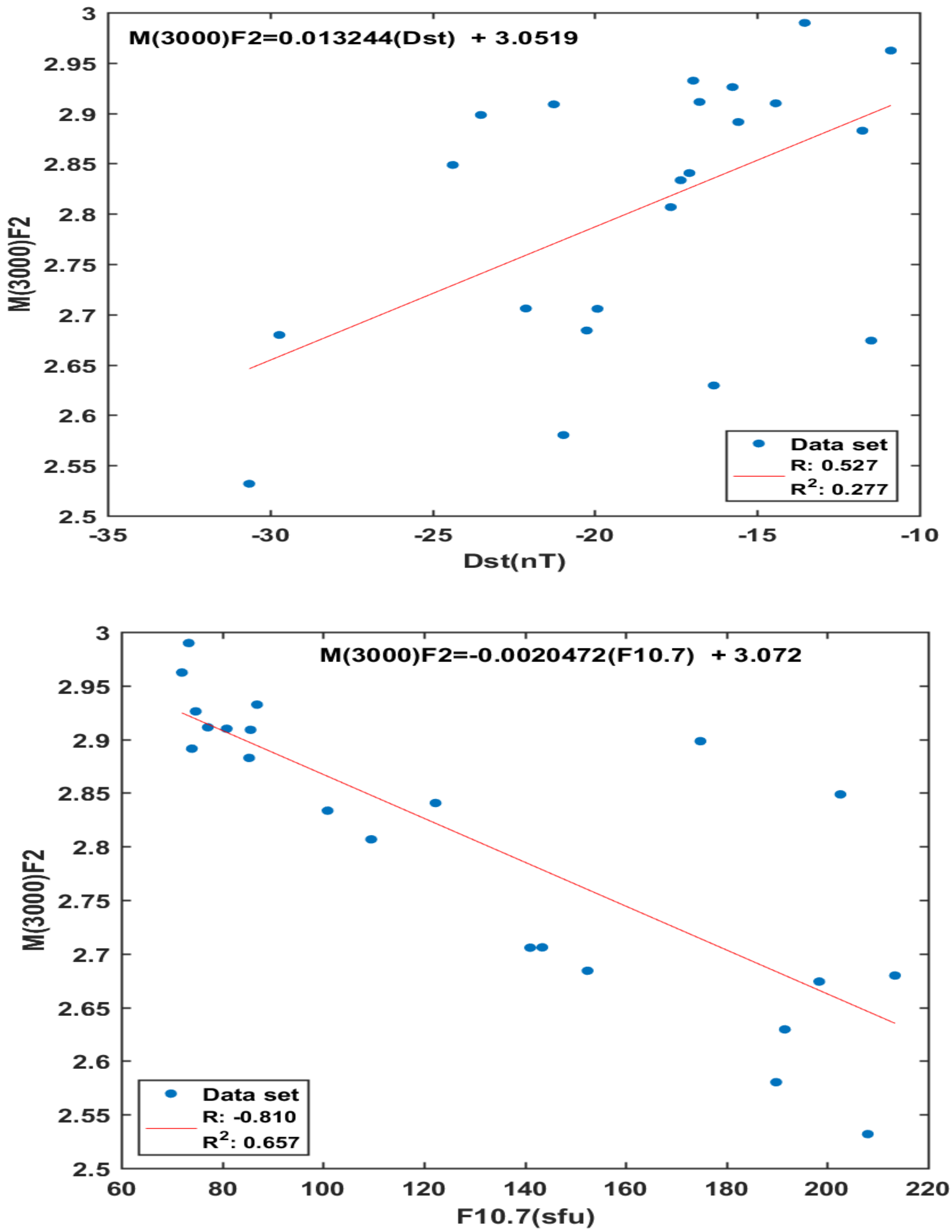

Figure 6a- The scatter plot of yearly average values of $M(3000)F2$ versus Dst (top panel), and $M(3000)F2$ versus $F10.7$ (bottom panel) for the year 1976-1997.

https://doi.org/10.5194/egusphere-2026-4526
Preprint. Discussion started: 20 August 2026

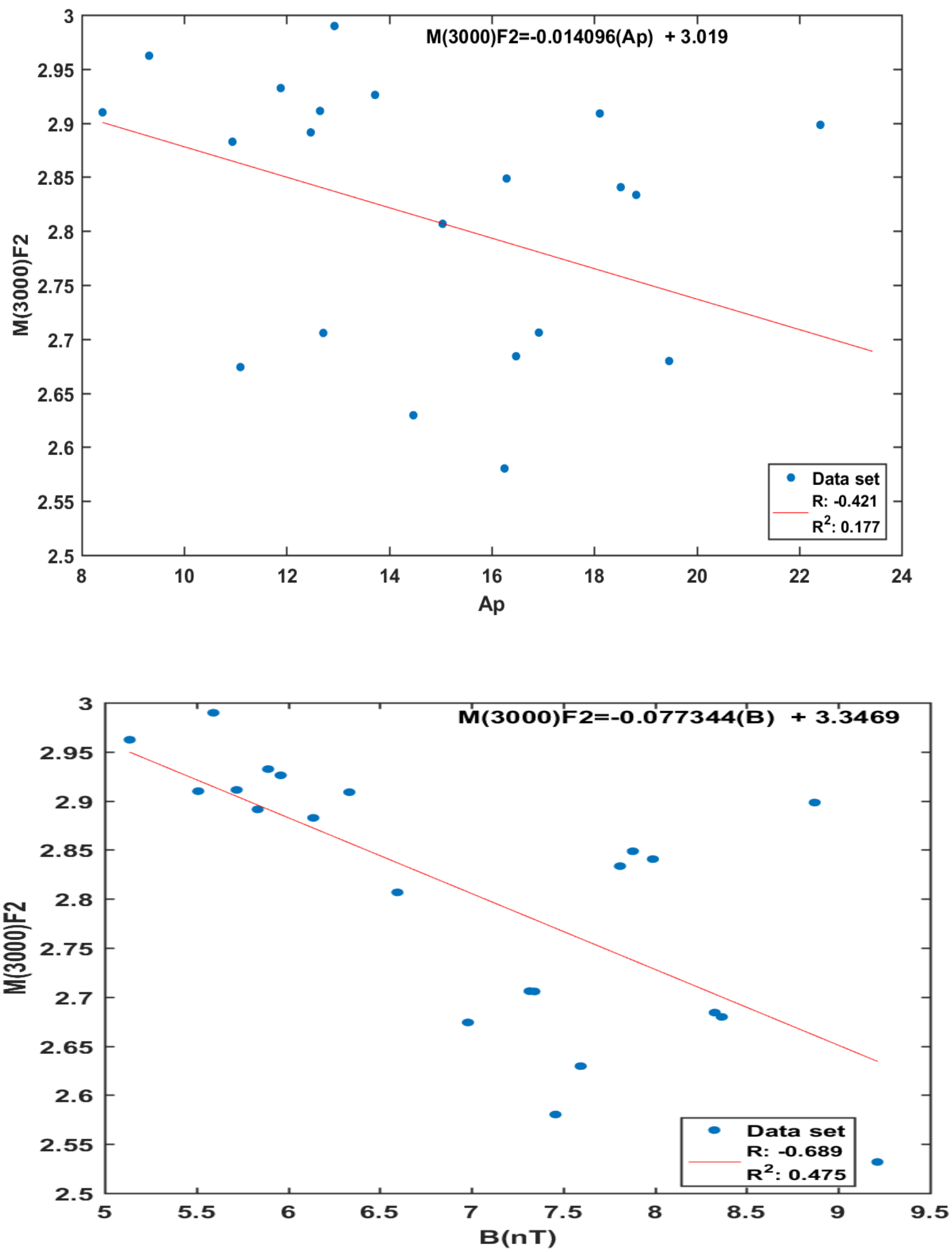

Figure 6b- The scatter plot of yearly average values of $M(3000)F2$ versus Ap (top panel), and $M(3000)F2$ versus B (bottom panel) for the year 1976-1997.

https://doi.org/10.5194/egusphere-2026-4526
Preprint. Discussion started: 20 August 2026

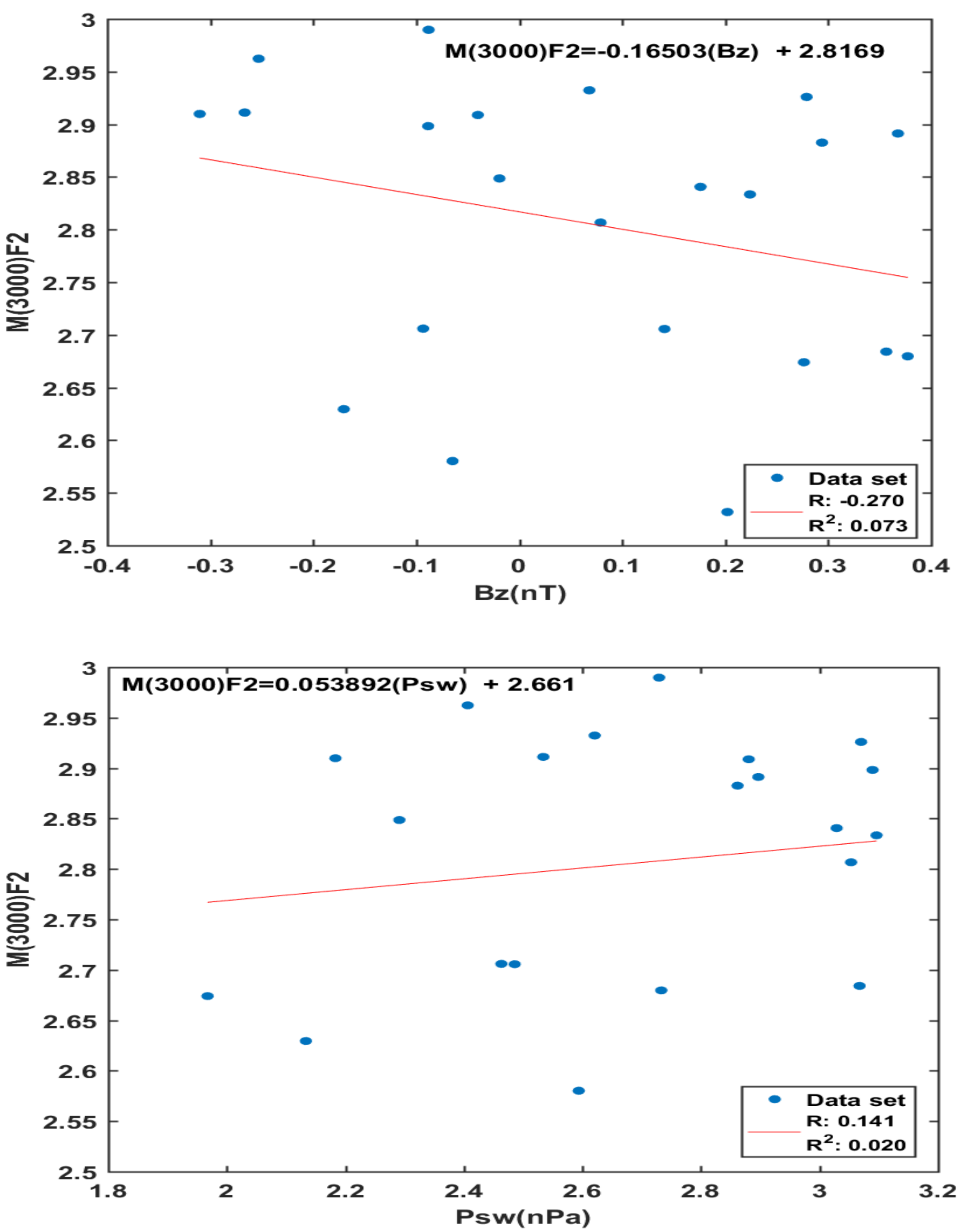

Figure 6c- The scatter plot of yearly average values of $M(3000)F2$ versus Bz (top panel), and $M(3000)F2$ versus Psw (bottom panel) for the year 1976-1997.

https://doi.org/10.5194/egusphere-2026-4526
Preprint. Discussion started: 20 August 2026

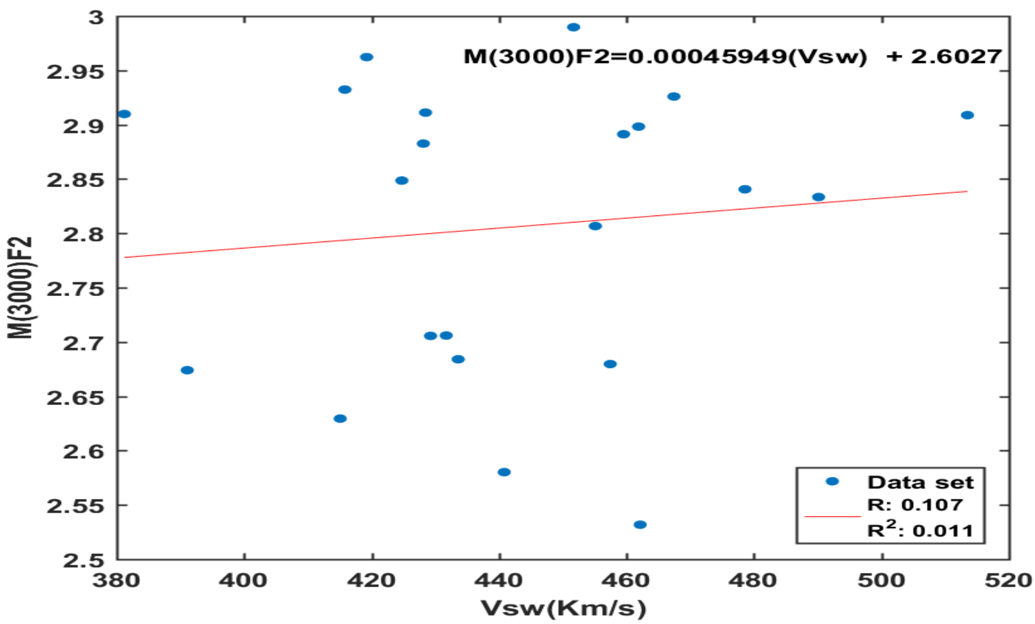

Figure 6d- The scatter plot of yearly average values of $M(3000)F2$ versus Vsw for the year 1976-1997.

https://doi.org/10.5194/egusphere-2026-4526
Preprint. Discussion started: 20 August 2026

Table 4: The Correlation coefficients (R), coefficients of determination (R^2), linear regression coefficients and p-values between M(3000)F2 and geophysical parameters over Ouagadougou during solar cycles 21-22.

Parameter	a	b×10^{-4}	R	R^2	Influence (%)	P-value	Statistical significance
B	3.347	-773.4	-0.689	0.475	47.5	3.91×10^4	Significant
Psw	2.661	-538.9	0.141	0.020	2.0	0.5314	Not significant
Bz	2.817	-1650.3	-0.270	0.073	7.3	0.2243	Not significant
Dst	3.052	132.4	0.527	0.277	27.7	0.0117	Significant
Vsw	2.603	4.595	0.107	0.011	1.1	0.6355	Not significant
F10.7	3.072	-20.47	-0.810	0.657	65.7	4.92×10^6	Significant
Ap	3.019	-141.0	-0.421	0.177	17.7	0.0510	Not significant

https://doi.org/10.5194/egusphere-2026-4526
Preprint. Discussion started: 20 August 2026

Discussion

4.1 Solar cycle, diurnal and seasonal variability of M(3000)F2

The observed diurnal variation of M(3000)F2 is primarily associated with changes in the height of the F2 layer (hmF2), since M(3000)F2 is inversely related to hmF2 (Dudeney, 1983). During daytime, enhanced solar EUV radiation increases ion production and strengthens the equatorial E × B plasma drift, lifting the F2 layer to higher altitudes. The resulting increase in hmF2 is accompanied by lower M(3000)F2 values around local noon and during the afternoon. After sunset, the weakening of the upward plasma drift, together with thermospheric winds and plasma diffusion, allows the F2 layer to descend gradually, producing the higher M(3000)F2 values observed during the nighttime and early morning hours. Similar diurnal behaviour has been reported in equatorial ionospheric studies by Abdu et al. (1990), Rishbeth and Mendillo (2001), and Oyekola and Fagundes (2012), who associated variations in F-region height with changes in equatorial electrodynamics and plasma transport.

A key finding of the present study is the inverse dependence of M(3000)F2 on solar activity, with the highest values occurring during the low solar activity year and the lowest during the high solar activity year. This behaviour reflects the sensitivity of M(3000)F2 to the vertical structure of the F2 layer rather than to electron density alone. During solar maximum, enhanced EUV radiation increases thermospheric heating and promotes greater uplift of the F2 layer, resulting in higher hmF2 values. Because M(3000)F2 decreases as hmF2 increases, lower values are expected during periods of enhanced solar activity despite the increase in ionisation. This inverse solar-cycle response agrees with earlier studies by Bilitza et al. (1979), Kouris (1998), and Oyekola and Fagundes (2012), all of which reported that M(3000)F2 exhibits an opposite solar-cycle dependence to electron-density parameters such as foF2.

The seasonal variations observed in this study further indicate that M(3000)F2 is influenced by changes in solar zenith angle, thermospheric circulation, and equatorial electrodynamics. The generally higher values recorded during the December solstice, together with the season-to-season differences observed under different levels of solar

https://doi.org/10.5194/egusphere-2026-4526
Preprint. Discussion started: 20 August 2026

activity, suggest that seasonal ionospheric dynamics are further modulated by the phase of the solar cycle. These variations are likely associated with seasonal changes in the vertical E × B plasma drift and thermospheric neutral winds, which influence the height and morphology of the F2 layer. Comparable seasonal characteristics have been reported for equatorial stations in the African sector by Oyekola and Fagundes (2012), while Kouris (1998) showed that seasonal variations in M(3000)F2 are governed primarily by changes in F-region structure rather than electron density alone. Collectively, these results indicate that the seasonal behaviour of M(3000)F2 over Ouagadougou reflects the combined influence of solar cycle variability and seasonal changes in equatorial ionospheric dynamics.

4.2 Relationship between M(3000)F2 and solar, solar wind and geomagnetic activity

The correlation and regression analyses demonstrate that M(3000)F2 responds differently to solar, solar wind, and geomagnetic forcing, indicating that these parameters contribute unequally to the long-term variability of the equatorial ionosphere over Ouagadougou. Among the investigated variables, the solar radio flux (F10.7) exhibits the strongest relationship with M(3000)F2 ($R = -0.810$, $R^2 = 0.657$, $p < 0.001$), indicating that approximately 65.7% of the observed interannual variability can be explained by changes in solar activity alone. This strong negative correlation confirms the inverse solar-cycle dependence identified in the seasonal and long-term analyses and demonstrates that increasing solar activity is associated with decreasing M(3000)F2.

The inverse relationship is physically consistent with the dependence of M(3000)F2 on the vertical structure of the F2 layer rather than on electron density alone. During periods of enhanced solar activity, increased EUV radiation raises thermospheric temperatures, modifies neutral composition, and enhances plasma transport, leading to an increase in the F2-layer peak height (hmF2). Since M(3000)F2 is inversely related to hmF2 (Dudeney, 1983), lower values are expected during solar maximum despite the increase in ionospheric ionisation. Similar inverse solar cycle behaviour has been reported by Bilitza et al. (1979), Kouris (1998), Oyekola and Fagundes (2010, 2012), and Bilitza

https://doi.org/10.5194/egusphere-2026-4526
Preprint. Discussion started: 20 August 2026

et al. (2022). The present results, therefore, provide further observational evidence that M(3000)F2 is primarily controlled by changes in F-region structure associated with solar activity.

The present findings also agree with earlier investigations over Ouagadougou by Oyekola and Fagundes (2010, 2012), who reported pronounced solar cycle and seasonal variability in M(3000)F2. However, the present study extends those investigations by simultaneously examining solar wind parameters and geomagnetic indices behaviour over two complete solar cycles and also studying the storm-time behaviour over the representative years. This broader approach provides a more comprehensive assessment of the geophysical processes governing M(3000)F2 over the African equatorial sector.

Among the solar wind parameters, the interplanetary magnetic field magnitude (B) shows the second strongest relationship with M(3000)F2 ($R = -0.689$, $R^2 = 0.475$, $p < 0.001$). Nearly half (47.5%) of the long-term variability in M(3000)F2 is associated with variations in IMF magnitude, suggesting that solar wind-magnetosphere coupling contributes substantially to modifications of the equatorial ionosphere. A statistically significant positive relationship was also obtained with the Dst index ($R = 0.527$, $R^2 = 0.277$, $p = 0.0117$), indicating that M(3000)F2 tends to be higher during relatively quiet geomagnetic conditions and decreases as geomagnetic disturbances become more intense. These results are consistent with the role of geomagnetic activity in modifying equatorial electrodynamics through prompt penetration electric fields, disturbance dynamo electric fields, thermospheric circulation, and composition changes, all of which influence the height and morphology of the F2 layer (Fejer, 2002; Pedatella and Liu, 2020).

Although Ap, Bz, solar wind dynamic pressure (Psw), and solar wind speed (Vsw) exhibited measurable correlations with M(3000)F2, none of these relationships reached statistical significance at the 95% confidence level ($p > 0.05$). The relatively low coefficients of determination (17.7%, 7.3%, 2.0%, and 1.1%, respectively) show that these parameters explain only a small fraction of the long-term variability in M(3000)F2. This does not necessarily imply

https://doi.org/10.5194/egusphere-2026-4526
Preprint. Discussion started: 20 August 2026

that they have no physical influence on the ionosphere. Rather, their effects are likely to be episodic and event-dependent, becoming more apparent during individual geomagnetic storms than in annual averages, where short-term fluctuations are substantially smoothed. In particular, the southward IMF component (Bz), although essential for initiating magnetic reconnection and geomagnetic storms, varies rapidly on timescales much shorter than those represented by yearly mean values.

Overall, the statistical and physical evidence indicate that solar activity is the dominant driver of long-term M(3000)F2 variability over Ouagadougou. In contrast, solar wind and geomagnetic processes provide secondary modulation through their influence on equatorial ionospheric electrodynamics. The results demonstrate that changes in the vertical structure of the F2 layer, controlled primarily by solar irradiance and modified by magnetosphere-ionosphere coupling, are the principal mechanisms governing long-term variations in M(3000)F2 over the African equatorial sector.

4.3 Storm-time response of M(3000)F2

The storm-time analyses demonstrate that M(3000)F2 over Ouagadougou responds sensitively to geomagnetic disturbances, with the most pronounced perturbations occurring during the main phase of the storms. In most of the events examined, M(3000)F2 decreased below the quiet-day average during the daytime, particularly between the late morning and afternoon hours. The magnitude and duration of the perturbations varied from one storm to another, reflecting differences in storm intensity, duration, seasonal conditions, and the background state of the equatorial ionosphere.

The observed daytime depletion of M(3000)F2 during the main phase is consistent with the well-established response of the equatorial F region to geomagnetic storms. During disturbed conditions, prompt penetration electric fields (PPEFs), disturbance dynamo electric fields (DDEFs), and storm-induced thermospheric circulation modify the vertical $E \times B$ plasma drift, producing changes in the height and structure of the F2 layer (Abdu et al., 1990; Fejer, 2002; Pedatella and Liu, 2020). Because M(3000)F2 is inversely related to the F2-layer peak height (hmF2)

(Dudeney, 1983), these storm-time electrodynamic processes produce the observed reductions and occasional enhancements in M(3000)F2 by altering the vertical structure of the equatorial ionosphere.

Although depletion dominated most of the analysed storms, periods of enhancement were also observed during the initial and recovery phases. Such enhancements are likely associated with transient penetration electric fields and favourable thermospheric wind conditions that temporarily increase the F-region height before disturbance dynamo effects become dominant. Similar storm-time enhancement-depletion patterns have been reported in previous investigations of equatorial ionospheric variability (Abdu et al., 1990; Fejer, 2002).

The recovery characteristics differed among the storm events. Some storms returned to near quiet-time conditions within one day, whereas others required two recovery days before M(3000)F2 approached the quiet-day profile. This variation indicates that recovery depends not only on storm intensity but also on the gradual restoration of thermospheric composition, neutral wind circulation, and ionospheric electrodynamics following geomagnetic disturbances.

Among the analysed events, the November 1991 superstorm (minimum Dst = -354 nT) produced one of the largest and most persistent perturbations, with substantial daytime depletion followed by a prolonged recovery. In contrast, the moderate storms generally produced smaller departures from the quiet-day average, although noticeable daytime reductions in M(3000)F2 were still observed. This behaviour suggests that stronger geomagnetic storms tend to produce larger and longer-lasting disturbances in the equatorial F-region propagation characteristics.

Overall, the storm-time results demonstrate that geomagnetic disturbances significantly modify the propagation factor M(3000)F2 over the African equatorial sector. The observed responses emphasise the importance of storm-induced electrodynamic processes in controlling F2-layer structure and HF radio wave propagation over Ouagadougou.

https://doi.org/10.5194/egusphere-2026-4526
Preprint. Discussion started: 20 August 2026

4.4 Implications for HF propagation and ionospheric modelling

The results of this study have important implications for HF radio communication and ionospheric modelling over the African equatorial sector. The demonstrated inverse dependence of M(3000)F2 on solar activity and its sensitivity to geomagnetic disturbances indicate that empirical propagation models should account for both long-term solar cycle variability and short-term storm-time electrodynamics. The long-term Ouagadougou ionosonde observations presented here also provide valuable validation data for improving empirical ionospheric models such as the International Reference Ionosphere (IRI), particularly over the data-sparse African equatorial region.

5. Conclusion

This study investigated the influence of solar activity, solar wind conditions, and geomagnetic activity on the ionospheric propagation factor M(3000)F2 over Ouagadougou, an equatorial station in the African sector, using long-term ionosonde observations spanning Solar Cycles 21 and 22 (1976-1997). The variability of M(3000)F2 was examined on diurnal, monthly, seasonal, solar cycle, and storm-time timescales, while correlation and linear regression analyses were used to evaluate its relationships with selected solar, solar wind, and geomagnetic parameters.

The analysis shows that M(3000)F2 exhibits pronounced diurnal variability, with high values during the nighttime and early morning hours and lower values during the daytime. Seasonal analyses reveal clear equinoctial and solstitial differences associated with variations in equatorial electrodynamics, thermospheric circulation, and solar forcing. A major finding is the inverse dependence of M(3000)F2 on solar activity, whereby the highest values occur during low solar activity and the lowest during high solar activity. This behaviour reflects the sensitivity of M(3000)F2 to the height and vertical structure of the F2 layer rather than to electron density alone.

https://doi.org/10.5194/egusphere-2026-4526
Preprint. Discussion started: 20 August 2026

The statistical analyses identify solar activity as the dominant driver of long-term M(3000)F2 variability. Among the investigated parameters, the solar radio flux (F10.7) exhibits the strongest statistically significant relationship with M(3000)F2 (R = -0.810, R^2 = 0.657), followed by the interplanetary magnetic field magnitude (B) (R = -0.689, R^2 = 0.475) and the Dst index (R = 0.527, R^2 = 0.277). By comparison, the relationships with Ap, Bz, solar wind dynamic pressure (Psw), and solar wind speed (Vsw) are weak and not statistically significant at the 95% confidence level, indicating that these parameters make comparatively small contributions to long-term variability.

Storm-time analyses further show that geomagnetic disturbances significantly influence M(3000)F2 over Ouagadougou. Most storm events were characterised by pronounced daytime depletion during the main phase, followed by gradual recovery over one or two days, depending on storm intensity and the prevailing ionospheric conditions. These responses are consistent with storm-induced changes in equatorial electrodynamics, likely involving prompt penetration electric fields, disturbance dynamo electric fields, and thermospheric circulation, which influence the height and structure of the F2 layer.

Overall, the results indicate that long-term variability in M(3000)F2 over the African equatorial sector is governed primarily by solar activity, while solar wind and geomagnetic processes provide important secondary modulation, particularly during disturbed periods. This study provides a comprehensive characterisation of the long-term behaviour of M(3000)F2 over Ouagadougou and improves understanding of the relative roles of solar activity, solar wind, and geomagnetic forcing in shaping equatorial ionospheric propagation. The findings also provide a valuable observational basis for improving HF radio wave propagation prediction, empirical ionospheric modelling, and space weather applications in the data-sparse African equatorial region.

Data availability: Data available on request.

https://doi.org/10.5194/egusphere-2026-4526
Preprint. Discussion started: 20 August 2026

Author contributions- The author conceived the study, performed the data analysis, interpreted the results, wrote the manuscript, and approved the final version.

Competing interests- The author declares that there are no competing interests.

Acknowledgements

The author is grateful to the host of the ionosonde equipment in Ouagadougou and the Centre National d'Etude des Télécommunications (CNET), France, for making the ionosonde data at Ouagadougou available for scientific work. He also acknowledges the Space Physics Data Facility (SPDF) at the Goddard Space Flight Centre for providing access to solar, solar wind, and geomagnetic data.

Note:

The author used a language editing tool (ChatGPT, OpenAI) to improve the clarity and readability of the manuscript. The authors are solely responsible for the content, editing, and interpretation of the results.

References

Abdu, M. A., Batista, I. S., and Bittencourt, J. A.: Some characteristics of the ionospheric F region at equatorial latitudes, *J. Geophys. Res.*, **95**, 17093–17102, 1990.

Bilitza, D., Sheikh, N. M., and Eyfrig, R.: A global model for the height of the F2 peak using M(3000)F2 values from the CCIR numerical maps, *Telecommunication Journal*, **46**, 549–553, 1979.

Bilitza, D.: International Reference Ionosphere 2000, *Radio Sci.*, **36**, 261–275, https://doi.org/10.1029/2000RS002432, 2001.

Bilitza, D.: IRI is the International Standard for the ionosphere, *Adv. Radio Sci.*, **16**, 1–11, https://doi.org/10.5194/ars-16-1-2018, 2018.

https://doi.org/10.5194/egusphere-2026-4526
Preprint. Discussion started: 20 August 2026

Bilitza, D., Pezzopane, M., Truhlik, V., Altadill, D., Reinisch, B. W., and Pignalberi, A.: The International Reference Ionosphere Model: A review and description of an ionospheric benchmark, *Rev. Geophys.*, **60**, e2022RG000792, https://doi.org/10.1029/2022RG000792, 2022.

Dudeney, J. R.: The accuracy of hmF2 deduced from M(3000)F2, *J. Atmos. Terr. Phys.*, **45**, 629–640, https://doi.org/10.1016/S0021-9169(83)80011-8, 1983.

Eleman, F.: The geomagnetic field, in: *Cosmical Geophysics*, edited by: Egeland, A., Holter, Ø., and Omholt, A., Universitetsforlaget, Oslo, 45–62, 1973.

Fejer, B. G.: Low-latitude ionospheric electrodynamics, *J. Atmos. Sol.-Terr. Phys.*, **64**, 1401–1408, https://doi.org/10.1016/S1364-6826(02)00054-7, 2002.

Gonzalez, W. D., Joselyn, J. A., Kamide, Y., Kroehl, H. W., Rostoker, G., Tsurutani, B. T., and Vasyliūnas, V. M.: What is a geomagnetic storm?, *J. Geophys. Res.*, **99**, 5771–5792, https://doi.org/10.1029/93JA02867, 1994.

Kazeem, A. K., Adeniyi, J. O., and Adediji, A. T.: Modelling of the equatorial ionospheric E layer based on cos χ index, *Indian J. Radio Space Phys.*, **43**, 205–212, 2014.

Kazeem, A. K., Olawepo, A. O., and Rabiu, A. B.: Variability of NmF2 and its correlation with solar and geomagnetic variations at an equatorial station in the African sector, *Indian J. Radio Space Phys.*, **49**, 180–196, 2020.

Kazeem, A. K., Rabiu, A. B., and Amory-Mazaudier, C.: Solar-geomagnetic activity effect on NmE over Ouagadougou, an equatorial anomaly station in the African sector, *J. Atmos. Sol.-Terr. Phys.*, **280**, 106756, https://doi.org/10.1016/j.jastp.2026.106756, 2026a.

https://doi.org/10.5194/egusphere-2026-4526
Preprint. Discussion started: 20 August 2026

Kazeem, A. K., Abe, O. E., Atijosan, A., and Yusuf, K. A.: Variability of solar wind parameters and their relationship with F10.7, Dst, Ap, and AE indices across Solar Cycles 21–24, *J. Atmos. Sol.-Terr. Phys.*, **283**, 106838, https://doi.org/10.1016/j.jastp.2026.106838, 2026b.

Klobuchar, J. A. and Doherty, P. H.: The correlation of daily solar flux values with total electron content, in: *Proceedings of the International Beacon Satellite Symposium*, edited by Lee, M.-C., Cambridge, Massachusetts, USA, Plasma Fusion Centre, Massachusetts Institute of Technology, 192–195, 1992.

Kouris, S. S.: The solar-cycle variation of M(3000)F2 and its correlation with that of foF2, *Ann. Geophys.*, **16**, 587–594, https://doi.org/10.1007/s00585-998-0587-1, 1998.

Ouattara, F., Amory-Mazaudier, C., Fleury, R., Lassudrie-Duchesne, P., Vila, P., and Petitdidier, M.: West African equatorial ionospheric parameters climatology, *Ann. Geophys.*, **27**, 2503–2514, https://doi.org/10.5194/angeo-27-2503-2009, 2009.

Oyekola, O. S. and Fagundes, P. R.: Variation in the ionospheric propagating factor M(3000)F2 at Ouagadougou, Burkina Faso, *Adv. Space Res.*, **46**, 74–80, https://doi.org/10.1016/j.asr.2010.02.017, 2010.

Oyekola, O. S. and Fagundes, P. R.: Equatorial M(3000)F2 estimation of F2-layer model peak heights during low solar activity, *Adv. Space Res.*, **49**, 711–715, https://doi.org/10.1016/j.asr.2011.11.031, 2012.

Pedatella, N. M. and Liu, H.: Ionospheric variability due to geomagnetic activity, *J. Geophys. Res. Space Physics*, **125**, e2019JA027674, https://doi.org/10.1029/2019JA027674, 2020.

Rabiu, A. B., Mamukuyomi, A. I., and Joshua, E. O.: Variability of the equatorial ionosphere inferred from geomagnetic field measurements, *Bull. Astron. Soc. India*, **35**, 607–618, 2007.

https://doi.org/10.5194/egusphere-2026-4526
Preprint. Discussion started: 20 August 2026

Rishbeth, H. and Mendillo, M.: Patterns of F2-layer variability, *J. Atmos. Sol.-Terr. Phys.*, **63**, 1661–1680, https://doi.org/10.1016/S1364-6826(01)00036-0, 2001.